



A novel analytical model to predict springback of DP780 steel based on modified Yoshida-Uemori two-surface hardening model

Hamid Hajbarati¹ · Asghar Zajkani¹

Received: 23 February 2018 / Accepted: 4 July 2018 / Published online: 2 August 2018
© Springer-Verlag France SAS, part of Springer Nature 2018

Abstract

Advanced high strength steels are widely used in the automotive industry due to their appropriate strength to weight ratio. This alloy has unique hardening behavior. In this paper, a novel analytical model is introduced to predict springback in U-shaped bending process of as-received and pre-strained DP780 dual phase steel specimens. This model is based on the Hill48 yield criterion and plane-strain condition. The effect of sheet thinning and the motion of the neutral surface is taken into account on the springback. The modified Yoshida-Uemori two surface hardening model is applied to investigate the effect of work hardening stagnation. This novel model is examined on the Numisheet 2011 benchmark 4. The effects of the blank holder force and work hardening stagnation are studied on the sheet springback phenomenon. By comparison of the present model with previous alternate models, obtaining the more accuracy is tangible. Also, it is demonstrated that the springback parameters have more changes with increasing the blank holder force. Also, the parameter of the work hardening stagnation has more effect on the pre-strained specimen as compared to the as-received sample.

Keywords Springback · Advanced high-strength steel · Yoshida–Uemori model · U-draw bending · Two-surface hardening model

Introduction

Springback is an undesired phenomenon during the forming process of metallic parts, which must be compensated in the optimization process. Material with the higher strength and lower modulus of elasticity have greater springback quantities. For example; advanced high-strength steels (AHSS) have more springback compared to conventional steels. Thus, multi-step forming processes are usually used in forming these alloys. Therefore, investigating the effect of pre-strain on the sequent forming operations of this material is significant. The U-shaped bending processes are used in the producing components such as channels, beams, and frames. In this process, sheet metals experience complex deformation, including stretch-bending, unbending and reverse bending. Therefore, after unloading in addition to the springback, the curvature of the sidewall will be seen. Accurate springback prediction in this forming process needs hardening models which can

consider complex behaviors of material in reverse loading stage. Various methods, including analytically, semi-analytical and finite element method (FEM) are used to predict springback of bending process. Analytical models can be used only for simple part geometries. FEM is time-consuming in comparison with the analytical methods and is sensitive to numerical parameters such as the type and size of the elements, integration scheme, yielding criterion and strain hardening rule.

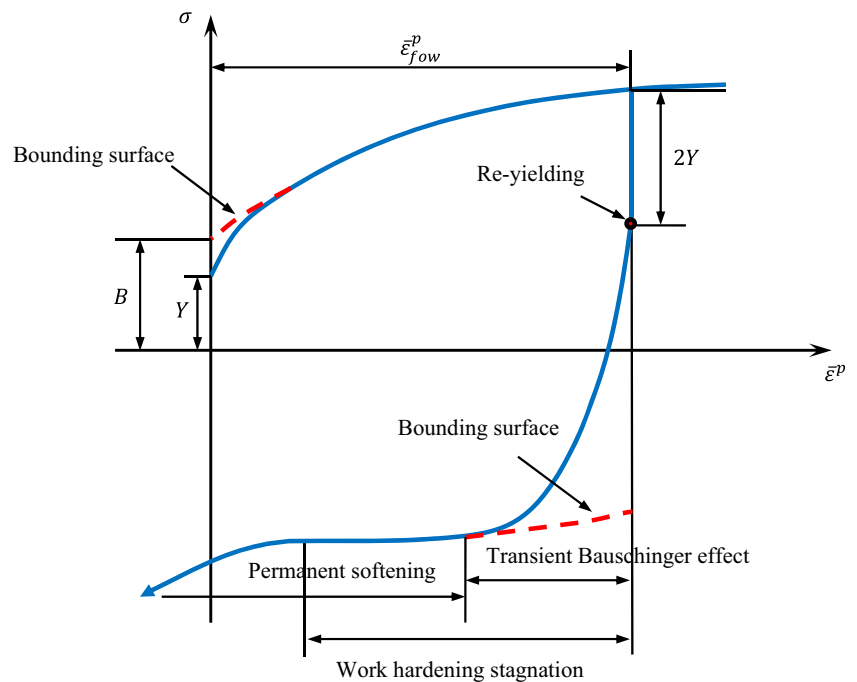
The accuracy of the springback prediction increases when the mechanical behavior is well described. So, the amount of springback depends on two main factors, namely; the stresses in the material before unloading and unloading modulus. The unloading modulus of the material is not constant and is a function of plastic strain. The mechanical behavior of materials in reverse loading due to reverse strain in the sheet metal forming process is highly regarded. Fig. 1 shows the flow stress curve on the outer surface of the sheet while bending around die arc and straightening process. Four features can be seen in this curve that includes: Bauschinger effect, transient behavior, permanent softening and work hardening stagnation.

Yoshida and Uemori introduced a hardening model be capable of reproducing the permanent softening, transient

✉ Hamid Hajbarati
h.hajbarati@gmail.com

¹ Department of Mechanical Engineering, Imam Khomeini International University, Qazvin, Iran

Fig. 1 The schematic of yield and bounding surface motion in a uniaxial forward-reverse loading [1]



Bauschinger effect and work hardening stagnation during large deformations [1]. In the category of two surface plasticity hardening models, only the Yoshida–Uemori model can capture work hardening stagnation. In this model, the relative kinematic motion of the yield surface concerning the bounding surface is a function of the difference between their sizes, and finally, it reaches to a saturated value. Thus, the yield surface never overpasses the bounding surface. The Yoshida–Uemori model can be used in a commercial finite element software to simulate the material behavior during the cyclic loading. In this case, Ghaei et al. introduced a semi-implicit and fully implicit integration scheme for implementation of the Yoshida–Uemori two-surface model into the finite element program and predicted the springback during the forming process [2, 3]. Hu et al. simulated the forming process and springback of an automobile body panel using JSTAMP/LS-DYNA and based on the Yoshida–Uemori constitutive model [4]. In addition, Zhang et al. simulated the stamping process using the LS-DYNA software and predicted springback for AHSS sheet based on the Yoshida–Uemori hardening model [5]. Also, Zhu et al. evaluated the accuracy of Yoshida–Uemori two-surface model in springback prediction after rotary-draw bending of the thin-walled rectangular H96 tube [6].

In past years a few studies have been introduced for analytical springback predictions in comparison with the finite element methods. Kagzi et al. developed an analytical model for springback prediction in bending of the bimetallic sheet based on Woo and Marshal constitutive equation and logarithmic strain [7]. Yi et al. proposed an analytical model based on residual differential strains between outer and inner surfaces

after elastic recovery [8]. In the case of a V-bending process, Yang et al. proposed a model to predict the springback in air-bending of AHSS, considering Young's modulus variation along with a piecewise hardening function [9]. Dong-Juan Zhang et al. proposed a method for sheet springback after V-bending based on Hill's yielding criterion and plane-strain condition [10]. In the case of the double curvature forming process, Parsa et al. presented an analytical model based on the moment-curvature relationships by considering changes of sheet thickness in double curved sheet metal forming method [11]. Zhang and Lin developed a solution of springback behavior of the sheet metals stamped by a rigid punch and an elastic die under plane-stress deformation [12]. Xue et al. established an analytical model based on the membrane theory of shells and an energy method after a double-curvature forming operation [13]. In the case of U-bending process, Pourboghrat and Chu described a technique to study the springback in the two-dimensional draw bending operation by using the moment-curvature relationships [14]. Dongjuan Zhang et al. established an efficient model on the Hill48 yielding criterion, plane-strain condition and the kinematic, isotropic and combined hardening rules to consider the springback after U-bending [15]. Nanu and Brabie presented a model for prediction of springback parameters during U stretch-bending process as a function of stresses distribution in the sheet thickness [16]. Jiang and Dai applied the isotropic hardening rule to investigate the time-dependent springback behaviors for an HSLA steel plate in the U-bending [17].

In previous analytical models, the energy method was used to calculate springback after U-shaped stretch-bending process. This method is based on the assumption of linear stress

distribution across sheet thickness while in reality, this assumption is not correct.

In previous papers, authors obtained the springback of a DP780 strip with and without pre-strain effects after U-shaped stretch bending process and explained the benchmark 4 of the Numisheet 2011 based on the energy method [18, 19]. These models were established on the anisotropic nonlinear kinematic (ANK) hardening model by considering the variation of material unloading modulus. Also, the Hill48 yielding criterion was used at the plane-strain condition as well as the material transverse isotropy. It was seen that considering the variable unloading modulus in these models causes reduction of the accuracy for the springback prediction as also reported by Yang et al. [9]. This event can be due to the plane-strain condition along with some simplifications, which were inserted in those solutions. Accordingly, in this paper, we present a novel analytical model based on the modified Yoshida-Uemori two-surface hardening model with the constant unloading modulus. The Hill48 yielding criterion is used based on the assumption of plane-strain condition and orthogonal axes of anisotropy. In this model, the change of the sheet thickness during unloading process is neglected. The effect of the work hardening stagnation and blank holder force on the springback of as-received and pre-strained specimens are investigated.

Material models

In this paper, the modified Yoshida-Uemori hardening model and Hill’s 1948 yielding criterion are used to analyze the material behavior of DP780 steel sheets. Also, the plane-strain condition is considered to calculate the sheet strains and stresses.

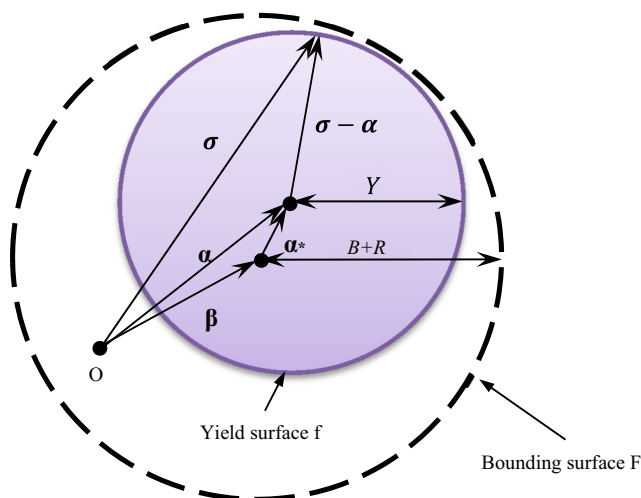


Fig. 2 Schematic of Yoshida-Uemori two surface model [1]

Theory of the modified Yoshida-Uemori two-surface hardening model

The model of Yoshida-Uemori is a revised model based on Chaboche model, which can capture phenomenon of the work hardening stagnation. This model assumes two surfaces; yield surface and boundary surface in which the yield surface develops within the bounding surface as shown in Fig. 2. The yield surface has kinematic hardening only while the bounding surface has both kinematic and isotropic hardening. Firstly, the associated flow rule for the yield surface is given by the following equation [1]:

$$f = \bar{\sigma}(\sigma - \alpha) - Y = 0 \tag{1}$$

Where σ and α denote the Cauchy stress deviator and center of yield surface, respectively. Also, Y is the size of yield surface. Moreover, the bounding surface can be described as follows:

$$F = \bar{\sigma}(\sigma - \beta) - (B + R) = 0 \tag{2}$$

Where β is the center of bounding surface, and B and R are the initial size of the bounding surface and isotropic hardening, respectively. The backstress α is considered as [1]:

$$\alpha = \alpha^* + \beta \tag{3}$$

Where α^* is the relative motion of the yielding surface concerning the bounding surface. Its rate can be calculated as follows [20]:

$$\dot{\alpha}^* = C_x \left(\frac{B + R \left(\frac{\bar{\epsilon}^p}{Y} \right) - Y}{Y} (\sigma - \alpha) - \alpha^* \right)^{\cdot p} \bar{\epsilon} \tag{4}$$

In above equation, C_x is a material parameter, and $\bar{\epsilon}^p$ is the equivalent plastic strain rate. Also, the kinematic hardening of the boundary surface is expressed as follows:

$$\dot{\beta} = k \left(\frac{b}{B + R \left(\frac{\bar{\epsilon}^p}{Y} \right)} (\sigma - \beta) - \beta \right)^{\cdot p} \bar{\epsilon} \tag{5}$$

In the modified Yoshida-Uemori hardening model proposed by Eggertsen and Mattiasson [20], the following assumptions are considered:

$$B = Y, \quad R \left(\frac{\bar{\epsilon}^p}{Y} \right) = \sigma \left(\frac{\bar{\epsilon}^p}{Y} \right) - \beta \left(\frac{\bar{\epsilon}^p}{Y} \right) - Y \tag{6}$$

The function $\sigma(\bar{\epsilon}^p)$ can be determined based on Swift hardening law as follows:

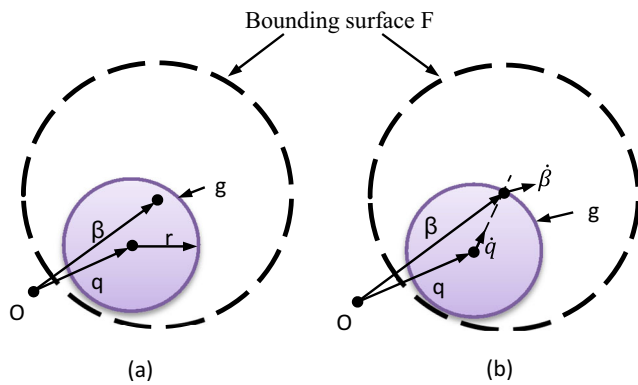


Fig. 3 Schematic of surface g in stress space. **a** Non-isotropic hardening ($\dot{R} = 0$); and **b** isotropic hardening ($\dot{R} > 0$) [1]

$$\sigma(\bar{\varepsilon}^p) = K(\varepsilon_0 + \bar{\varepsilon}^p)^n \tag{7}$$

where K and n are the parameters of the Swift hardening equation as are equal to $K = 1280.23 \text{ Mpa}$ and $n = 0.146$, respectively [21]. Also, the value of the parameter ε_0 for $Y = 527 \text{ Mpa}$ is equal to 0.00229.

Besides, the stresses during the uniaxial forward tensile loading can be calculated as follows [20]:

$$\begin{cases} \beta_{fowt} = b \left(1 - e^{-k\bar{\varepsilon}^p} \right) \\ \alpha_{fowt} = \sigma \left(\bar{\varepsilon}^p \right) - Y \\ \sigma_{fowt} = \sigma \left(\bar{\varepsilon}^p \right) \end{cases} \tag{8}$$

Alternately, during the uniaxial reverse compressive loading, we have:

$$\begin{cases} \alpha_{revc}^* \approx -R \left(\bar{\varepsilon}^p \right) + \left(\alpha_x^{*0} + R \left(\bar{\varepsilon}^p \right) \right) e^{-c_x \left(\bar{\varepsilon}^p - \bar{\varepsilon}_0^p \right)} \\ \beta_{revc} \approx \frac{b(-Y + \alpha_x^*)}{Y + R \left(\bar{\varepsilon}^p \right)} + \left(\beta_x^0 - \frac{b(-Y + \alpha_x^*)}{Y + R \left(\bar{\varepsilon}^p \right)} \right) e^{-k \left(\bar{\varepsilon}^p - \bar{\varepsilon}_0^p \right)} \\ \alpha_{revc} = \alpha_x^* + \beta_x \\ \sigma_{revc} = -Y + \alpha_x \end{cases} \tag{9}$$

Corresponding to above procedure during the reverse loading, it can be seen that σ_x tends toward $\sigma(\bar{\varepsilon}^p)$ for the large values of $\bar{\varepsilon}^p$. This fact indicates that the above equations cannot comprise the permanent softening and the phenomenon of the work hardening stagnation. For this purpose, Yoshida and Uemori proposed an additional surface by g in the stress space as shown in Fig. 3 with the following equation [1]:

$$g = \bar{\sigma}(\sigma - q) - r = 0 \tag{10}$$

Where q and r denote the center and size of the surface, respectively. It is assumed that the center of the bounding

surface β exists either on or inside the surface g . In addition, the isotropic hardening of the bounding surface (R) takes place when tensor of β remains on the surface g as shown in Fig. 3(b) which means:

$$\begin{aligned} g &= \bar{\sigma}(\beta - q) - r = 0 \\ \frac{\partial g}{\partial \beta} : \dot{\beta} &> 0 \end{aligned} \tag{11}$$

If the above condition is satisfied, then $\dot{R} > 0$; otherwise $\dot{R} = 0$. The kinematic hardening of the surface g is defined as [1]:

$$\dot{q} = \dot{\mu}(\beta - q) \tag{12}$$

With:

$$\dot{\mu} = \frac{\Gamma - r}{r} \tag{13}$$

$$\dot{\Gamma} = \frac{\partial \bar{\sigma}(\beta, q)}{\partial \beta} : \dot{\beta} \tag{14}$$

Also, the isotropic hardening of surface g is defined as follows:

$$\dot{r} = h \dot{\Gamma} \quad \text{when} \quad \dot{R} > 0 \tag{15}$$

$$\dot{r} = 0 \quad \text{when} \quad \dot{R} > 0 \tag{16}$$

Where $0 \leq h \leq 1$ is a material parameter.

If the center of the bounding surface stays on the surface g then:

$$r = \beta - q \tag{17}$$

And:

$$\dot{\mu} = \frac{(1-h)\Gamma}{r} \tag{18}$$

In the following procedure, by including stretching, compressive bending and straightening, the effect of work hardening stagnation will be investigated during one loading cycle. By substituting Eq. (17) into Eq. (14), the following equation can be obtained during stretching process:

$$\dot{\Gamma} = \dot{\beta} \tag{19}$$

By substituting Eqs. (18) and (19) into Eq. (12), we have:

$$\dot{q} = (1-h)\dot{\beta} \tag{20}$$

Moreover, by substituting Eq. (19) into the Eq. (15), the following equation can be obtained for the stretching process:

$$\dot{r} = h \dot{\beta} \tag{21}$$

The work hardening stagnation stops during the reverse compressive loading when the following condition is satisfied:

$$\beta_{revc}^{whs} = -r + q \tag{22}$$

In above equation, β_{revc}^{whs} is equal to the critical value which the work hardening process starts after reaching β_{revc} to its value. By substituting Eqs. (20) and (21) in the above equation, the following critical value can be obtained:

$$\beta_{revc}^{whs} = (1-2h)\beta_{fowt} \tag{23}$$

Moreover, the following equations will be obtained during the compressive bending:

$$\dot{r} = -h \dot{\beta} \tag{24}$$

$$\dot{q} = (1-h) \dot{\beta} \tag{25}$$

After the work hardening process, the center and radius of surface g can be updated by integrating the Eqs. (24) and (25) as follows:

$$r = h\beta_{fowt} - h(\beta_{revc} - \beta_{revc}^{whs}) \tag{26}$$

$$q = (1-h) \cdot \beta_{fowt} + (1-h) \cdot (\beta_{revc} - \beta_{revc}^{whs}) \tag{27}$$

During the straightening stage after compressive bending, the following critical value for β_{revt}^{whs} can be obtained:

$$\beta_{revt}^{whs} = r + q = \beta_{fowt} + (1-2h) \cdot (\beta_{revc} - \beta_{revc}^{whs}) \tag{28}$$

Where β_{revt}^{whs} is equal to a critical value. The work hardening process starts after reaching β_{revt} to that. The parameters of the modified Yoshida-Uemori model are given in Table 1 for DP780.

Hill's 1948 yielding criterion

In the previous model, however, the blank was considered with the transverse isotropy while in this model, the axes of material anisotropy are assumed to be orthogonal. By neglecting the shear stresses and ($\sigma_r = 0$), the Hill48 yield criterion can be expressed as follows [23]:

$$F\sigma_z^2 + G\sigma_\theta^2 + H(\sigma_\theta - \sigma_z)^2 = \bar{\sigma}^2 \tag{29}$$

Differentiating both sides of Eq. (29) and considering $d\bar{\sigma} = 0$ leads to write:

$$\frac{d\sigma_z}{d\sigma_\theta} = \frac{(G + H)\sigma_\theta - H\sigma_z}{H\sigma_\theta - (F + H)\sigma_z} \tag{30}$$

According to the principle of plastic normality, we have:

$$\frac{d\varepsilon_z}{d\varepsilon_\theta} = -\left(\frac{d\sigma_z}{d\sigma_\theta}\right)^{-1} = \frac{\varepsilon_z}{\varepsilon_\theta} \tag{31}$$

Thus:

$$\frac{\varepsilon_z}{\varepsilon_\theta} = \frac{(F + H)\sigma_z - H\sigma_\theta}{(G + H)\sigma_\theta - H\sigma_z} \tag{32}$$

Since $\varepsilon_z = 0$, the following relation will be obtained:

$$\sigma_z = \frac{H}{H + F} \sigma_\theta \tag{33}$$

Substituting the above equation into the yield function results

$$\bar{\sigma} = \frac{|\sigma_\theta|}{C_h} \tag{34}$$

Where $C_h = \frac{(H + F)}{\sqrt{(F + G)H^2 + 2FGH + (G + H)F^2}}$ is the hardening parameter. Based on the equivalent plastic work principle, we have:

$$\bar{\sigma} d\bar{\varepsilon}^p = \sigma_\theta d\varepsilon_\theta + \sigma_z d\varepsilon_z \tag{35}$$

Substituting Eq. (34) and considering ($d\varepsilon_z = 0$) in the previous equation leads to:

$$\frac{d\bar{\varepsilon}^p}{\bar{\varepsilon}} = C_h |\varepsilon_\theta| \tag{36}$$

The value of the constants in Eq. (29) are provided in the benchmark material data sheet and are $F = 0.4640$, $G = 0.5615$, and $H = 0.4385$.

Analysis of the sheet stretch-bending process

In this section, the general assumptions which are considered in the sheet deformation analysis are described. Also, an approach for determining the sheet stretching force and strain through the sheet thickness is introduced.

General assumptions

Deformation of the sheet at the edges of the punch and die can be considered as a stretch-bending process as shown in Fig. 4 with examining the following assumptions:

Table 1 Material parameters of the Yoshida-Uemori model for DP780 [22]

Parameter	C_x	$b(Mpa)$	k	h	$Y(Mpa)$	$\bar{\epsilon}_{lim}$	$E(Gpa)$	ν
value	137.9	165.7	29.1	0.99	527	0.198	198.8	0.3

1. The shear stresses in the sheet thickness can be neglected.
2. The principal direction for stresses and strains are considered along with the sheet thickness, width, and the length.
3. According to the plane strain condition, the strains in the width direction of the sheet are zero ($\epsilon_z = 0$).
4. The stress in the radial direction (σ_r) can be neglected.
5. Volume conservation law during the stretch-bending process is considered.
6. During the stretch-bending process, the sheet thickness is assumed to be equal at all cross-sections of the die and punch corners.
7. During the unloading process, the change of the sheet thickness is neglected.
8. During reverse bending process, the sheet thickness and the tensile force in sidewall section remains unchanged.

Determination of the sheet thickness

The strains must be determined to calculate the stresses through sheet thickness. For this purpose, the thickness of the sheet in different regions must be calculated. Determination of the sheet thickness is based on the

equilibrium equations. The stretching force in areas IV, II and III as shown in Fig. 4 can be calculated with the following equations [15]:

$$F_{IV} = \mu P_{bh} e^{\mu\phi} \tag{37}$$

$$F_{III} = F_C \tag{38}$$

$$F_{II} = F_C e^{-\mu\phi} \tag{39}$$

In above equations, μ is the friction coefficient between the tools and sheet, P_{bh} is the blank holder force. Also, ϕ represents the angular position of each cross-section at regions IV and II be relative to points B and E as shown in Fig. 4. The distribution of the tensile force throughout the sheet thickness can be obtained by using the above equations, and therefore the width of the sheet can be calculated.

Calculating the strains through the sheet thickness

According to the geometric relation which is shown in Fig. 5, the following equation can be obtained [15]:

$$\frac{R_n}{R_m} = \frac{t}{t_0} \tag{40}$$

Where R_n and R_m are the curvature radiuses of the neutral and middle surface of the sheet, respectively. Furthermore, t and t_0 represent the sheet thickness after and before stretch-bending process.

According to assumption (3), the strain at the width direction is zero ($\epsilon_z = 0$). Also, the tangential engineering strain at curvature radius (r) among the thickness is then achieved by the following equation:

$$\epsilon_\theta = \frac{r}{R_n} - 1 \tag{41}$$

For the pre-strained blanks, the value of the initial thickness can be obtained based on the assumption (5) as follows:

$$t_0 = (1 - \epsilon_\theta^{pre}) t_0 \tag{42}$$

In Eq. (42), the parameter ϵ_θ^{pre} is equal to the amount of plastic strain after the pre-strain process. As illustrated, the sheet is stretched firstly under a tensile force applied by the punch and then bent around the die radius. During the progressive loading, the equivalent plastic strain caused by bending around the die or punch corner can be expressed based on Eqs. (41) and (36) as follows:

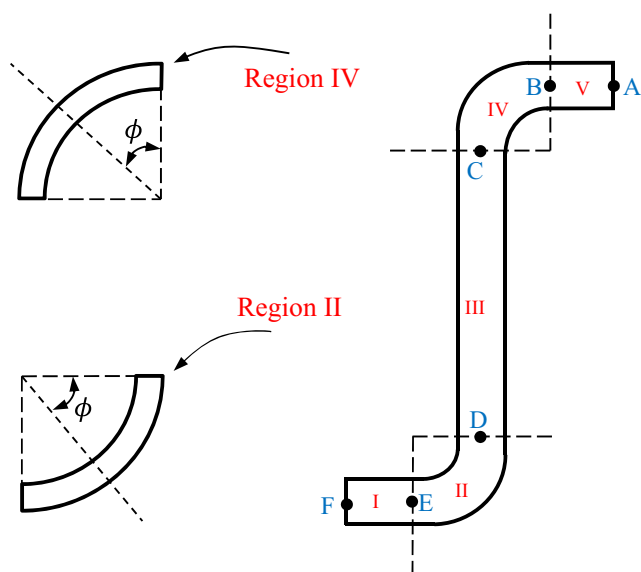
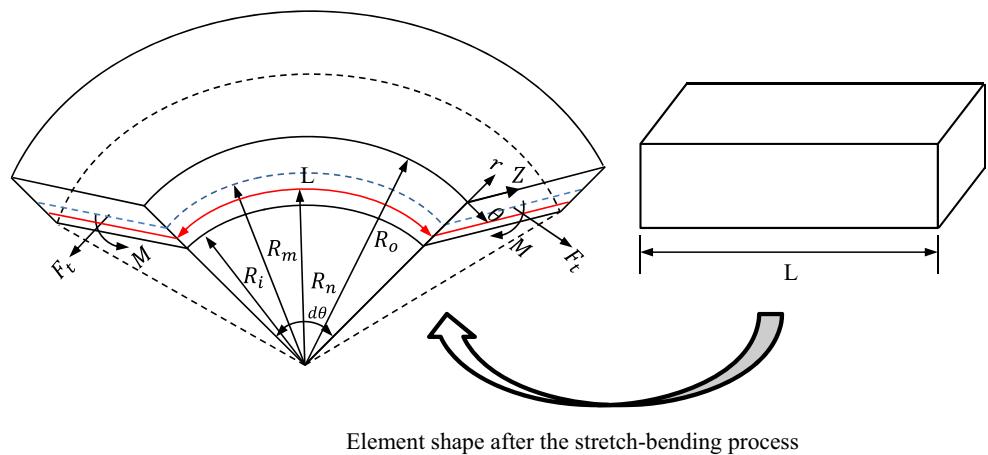


Fig. 4 Scheme of different sheet sections after U-shaped stretch-bending process

Fig. 5 The schematic of a small element located in die or punch corner during the stretch-bending process



$$\frac{p}{\bar{\epsilon}_{fow}} = |C_h \epsilon_\theta| - \bar{\epsilon}_{yield} + \bar{\epsilon}^{pre} = \left| C_h \left(\frac{r}{R_n} - 1 \right) \right| - \bar{\epsilon}_{yield} + \bar{\epsilon}^{pre} \quad (43)$$

In this equation, $\bar{\epsilon}^{pre} = C_h \epsilon_\theta^{pre}$. Also, $\bar{\epsilon}_{yield}$ is equal to the strain at which the material yields during the forward loading process after the pre-stretch process. It can be calculated respectively for tensile and compressive forward loading by:

$$\frac{t}{\bar{\epsilon}_{yield}} = \frac{K C_h (\epsilon_0 + \bar{\epsilon}^{pre})^n}{E_1} \quad (44)$$

$$\frac{c}{\bar{\epsilon}_{yield}} = \frac{C_h (-Y + \alpha (\bar{\epsilon}^{pre}))}{E_1} \quad (45)$$

In these equations, $E_1 = E/(1 - \nu^2)$ is elastic modulus in the plane strain condition, and ν is Poisson’s ratio.

After separation from the contact surface, the sheet will be straightened and enters the sidewall section as shown in Fig. 6. During this process, there is a reverse tangential strain, which is equal to the forward tangential strain. The equivalent plastic strain during the reverse loading process can be expressed as follows:

$$\frac{p}{\bar{\epsilon}_{rev}} = C_h \left| \left(\frac{r - R_n}{R_n} \right) \right| - \frac{2 C_h Y}{E_1} + \frac{p}{\bar{\epsilon}_{fow}} \quad (46)$$

Calculation of sheet springback after U-shaped bending

The non-uniform distribution of stress in the cross-section of the layer leads to deform and create springback during unloading. The sheet U-shaped bending springback occurs

in the regions II, III and IV, while regions I and V remain straight before and after unloading.

Accordingly, the change of the tangential stress after unloading process can be calculated with:

$$\Delta \sigma_\theta = E_1 \Delta \epsilon_\theta = E_1 (\epsilon_\theta^{ub} - \epsilon_\theta^b) \quad (47)$$

The tangential strain during the bending process can be calculated as follows:

$$\epsilon_\theta^b = \frac{r - R_n}{R_n} = \frac{z + R_m - R_n}{R_n} \quad (48)$$

In which the parameter z as shown in Fig. 7 is defined as:

$$z = r - R_m = r' - R'_m \quad (49)$$

Where the parameters r' and R'_m are contributed to the situation after unloading stage. Also, the tangential strain during the unloading process (ϵ_θ^{ub}) can be calculated as follows:

$$\epsilon_\theta^{ub} = \frac{r' - R'_n}{R'_n} = \frac{z + R'_m - R'_n}{R'_n} \quad (50)$$

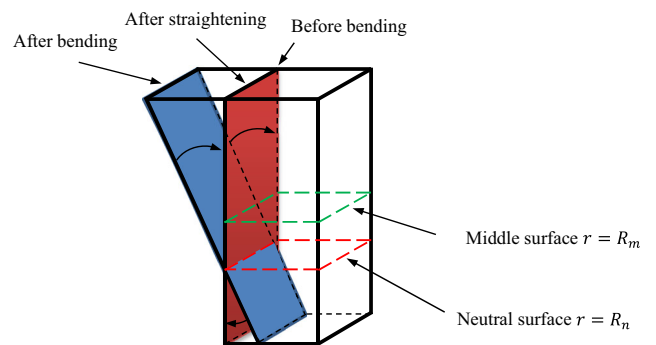
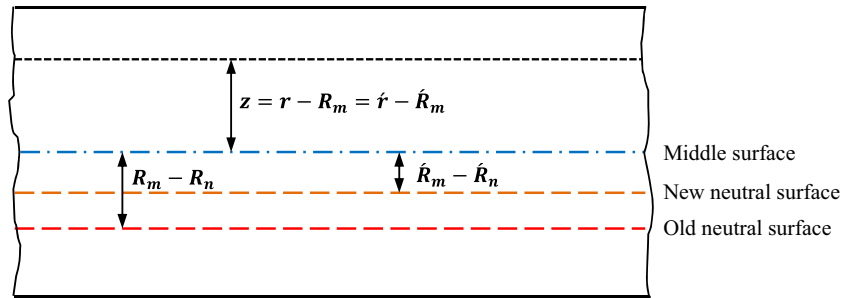


Fig. 6 The shape of a small element located at point C of sidewall section during the straightening process

Fig. 7 The relation between different parameters before and after unloading



Where parameters R'_m and R'_n are respectively equal to:

$$R'_m = \frac{R_m \pi}{\pi + 2\Delta\theta} \tag{51}$$

$$R'_n = \frac{R_n \pi}{\pi + 2\Delta\theta} \tag{52}$$

The change of the bending moment can be calculated as follows:

$$\Delta M = w \int_{-\frac{t}{2}}^{\frac{t}{2}} \Delta\sigma_{\theta} z dz = w \int_{-\frac{t}{2}}^{\frac{t}{2}} E_1 \left(\frac{1}{R'_n} - \frac{1}{R_n} \right) z^2 dz \tag{53}$$

The parameter w in Eq. (53) is equal to the width of the sheet and $\Delta M = -M$. Thus the change of the curvature radius can be calculated as follows:

$$\Delta \left(\frac{1}{R_n} \right) = \frac{-M}{w \int_{-\frac{t}{2}}^{\frac{t}{2}} E_1 z^2 dz} \tag{54}$$

The bending angle is equal to:

$$\theta = \frac{L}{R_n} \tag{55}$$

where L is equal to arc length. The bending angle change $\Delta\theta$ can be calculated with:

$$\Delta\theta = L \Delta \left(\frac{1}{R_n} \right) = \frac{-MR_n \frac{\pi}{2}}{w \int_{-\frac{t}{2}}^{\frac{t}{2}} E_1 z^2 dz} \tag{56}$$

Finally, the bending moment can be calculated as follows:

$$M = w \int_{R_i}^{R_o} \sigma_{\theta}^{fow} (r - R_m) dr \tag{57}$$

In the above equation, the bending moment is calculated at cross-section with $\phi = \pi/4$ from the punch and die corner.

Calculating the tangential stress of sheet cross-sections

In this section, firstly the thickness of the sheet during the stretch-bending process will be obtained. Then, the approach for estimating the bending moment and springback parameters will be discussed in the sidewall section of the sheet.

Punch and die edge sections

According to Eqs. (1), (7) and (43) the tangential stress distribution (σ_{θ}^{fow}) in the thickness direction can be expressed by the following equations:

$$\sigma_{\theta}^{fow} = \begin{cases} K C_h \left(\varepsilon_0 + \bar{\varepsilon}_{fow}^p \right)^n & R_n + c_t < r \leq R_o \\ E_1 \frac{r - R_n}{R_n} & R_n - c_c \leq r \leq R_n + c_t \\ C_h \left(-Y + \alpha \left(\bar{\varepsilon}_{fow}^p \right) \right) & R_i \leq r < R_n - c_c \end{cases} \tag{58}$$

Where c_t and c_c are the thickness of the elastic region in tensile and compressive stress zones respectively during the forward loading, as follow:

$$c_t = R_n \cdot \bar{\varepsilon}_{yield}^t \tag{59}$$

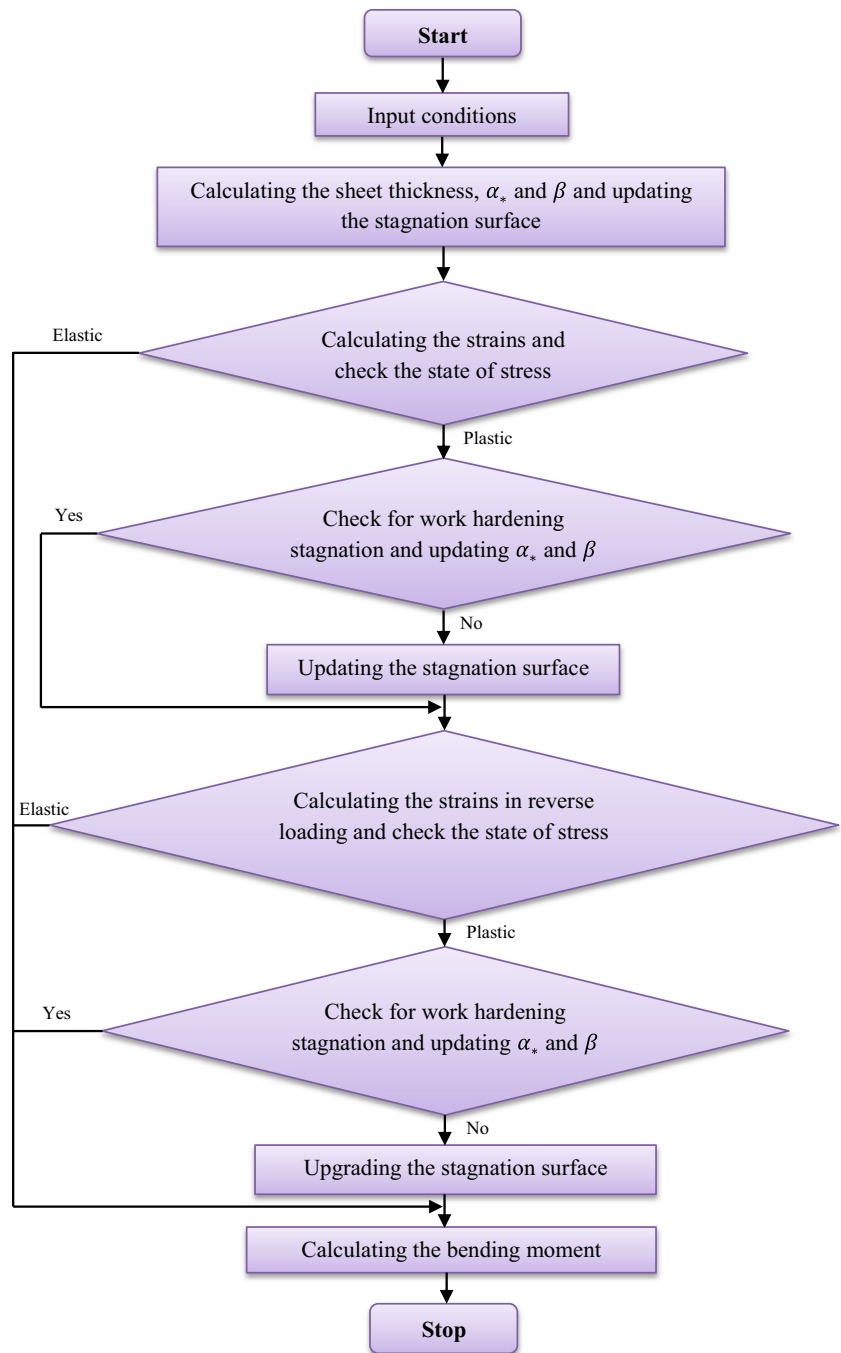
$$c_c = R_n \cdot \bar{\varepsilon}_{yield}^c \tag{60}$$

The sheet tensile force can be obtained by substituting Eq. (58) into the following equation:

$$F = w \int_{R_i}^{R_o} \sigma_{\theta}^{fow} \cdot dr \tag{61}$$

The thickness of the sheet after stretch-bending can be determined using Eqs. (61) and (37). Finally, the radius of the neutral surface, tangential strain, and stress

Fig. 8 Flowchart used in the calculation of sidewall bending moment



distribution can be achieved by using Eqs. (40), (41) and (58).

$$\left| \frac{r-R_n}{R_n} \right| - \frac{2Y}{E_1} = 0 \tag{62}$$

The sidewall section

During the reverse loading process material, the yield occurs when $\bar{\epsilon}_{rev}^p = \bar{\epsilon}_{low}^p$; Thus, the curvature radius in which the material yield occurs during the reverse compressive and tensile loading (R_y^{rc}, R_y^{rt}) can be obtained by solving the following equation:

The thickness of the sheet can be divided into three sub-intervals to calculate the tangential stress in the reverse loading process as follows:

- 1) Sub-interval (a): $R_i < r < R_n - c_c$

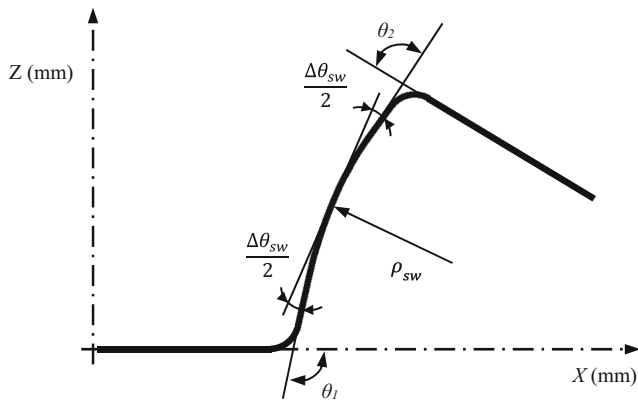


Fig. 9 Schematic for springback measurement method

$$\sigma_{\theta}^{sw} = \begin{cases} C_h \left[Y + \alpha \left(\frac{p}{\bar{\epsilon}_{rev}} \right) \right] & R_i < r < R_y^{rt} \\ \sigma_{\theta}^{ow} + E_1 \left(\frac{R_n - r}{R_n} \right) & R_y^{rt} < r < R_n - c_c \end{cases} \quad (63)$$

2) Sub-interval (b): $R_n - c_c < r < R_n + c_t$

$$\sigma_{\theta}^{sw} = 0 \quad (64)$$

3) Sub-interval (c): $R_n + c_t < r < R_o$

$$\sigma_{\theta}^{sw} = \begin{cases} \sigma_{\theta}^{ow} + E_1 \left(\frac{R_n - r}{R_n} \right) & R_n + c_t < r < R_y^{rc} \\ C_h \left[-Y + \alpha \left(\frac{p}{\bar{\epsilon}_{rev}} \right) \right] & R_y^{rc} < r < R_o \end{cases} \quad (65)$$

The change of the tangential stress of the sidewall section can be achieved from:

$$\Delta \sigma_{\theta}^{sw} = E_1 \left(\frac{z}{\rho_{sw}} \right) \quad (66)$$

Also, the change of the sidewall bending moment can be calculated from:

$$\Delta M = w \int_{-\frac{t}{2}}^{\frac{t}{2}} \Delta \sigma_{\theta}^{sw} z dz = w \int_{-\frac{t}{2}}^{\frac{t}{2}} E_1 \left(\frac{z}{\rho_{sw}} \right) z dz \quad (67)$$

where $\Delta M = -M_{sw}$, and parameter M_{sw} is equal to:

$$M_{sw} = w \int_{R_i}^{R_o} \sigma_{\theta}^{sw} (r - R_m) dr \quad (68)$$

Thus the final curvature radius of the sidewall can be calculated by using the following expression:

$$\rho_{sw} = - \frac{w \int_{-\frac{t}{2}}^{\frac{t}{2}} E_1 z^2 dz}{M_{sw}} \quad (69)$$

In the above equation, the sidewall bending moment (M_{sw}) is calculated at the die corner cross-section with $\phi = \pi/2$. The bending angle of the sidewall section after unloading process can be obtained with:

$$\Delta \theta_{sw} = \frac{L_{sw}}{\rho_{sw}} \quad (70)$$

Equations (53) and (68) can't be integrated analytically. Thus, a Simpson type numerical integration method is used for this purpose. The appropriate algorithm which is used to calculate the bending moment is shown in Fig. 8.

θ_1 , θ_2 , and ρ_{sw} are springback parameters which are shown in Fig. 9. Supposing the springback angle of regions II and III and IV, are equal to $\Delta \theta_1$ and $\Delta \theta_{sw}$ and $\Delta \theta_2$ respectively angles θ_1 and θ_2 can be calculated with the following equation [15]:

$$\theta_1 = 90^\circ + \Delta \theta_1 + \frac{\Delta \theta_{sw}}{2} \quad (71)$$

$$\theta_2 = 90^\circ + \Delta \theta_2 - \frac{\Delta \theta_{sw}}{2} \quad (72)$$

Fig. 10 A schematic of Numisheet2011 benchmark problem 2-D draw bending

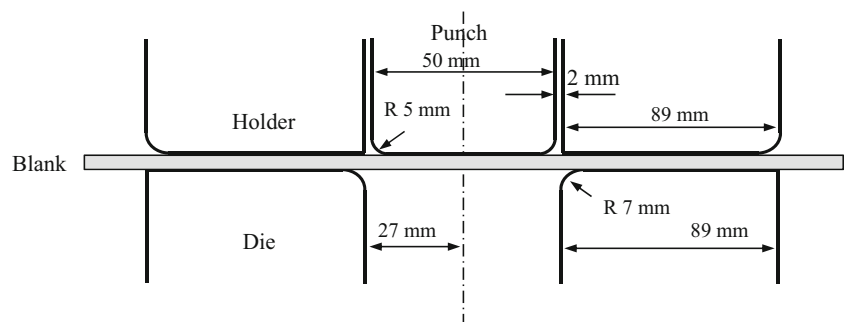


Table 2 The comparison between the results obtained from present and previous analytical model with experimental data

Without pre-strain						
Hardening model	Yield criterion	Solution method	$\theta_1(^{\circ})$	$\theta_2(^{\circ})$	$\rho_{sw}(mm)$	Average error %
		Experimental [25]	115.8	79.2	118.2	
ANK	Hill48	Previous model [19]	113.7	77.6	106.4	4.6
YU	Hill48	Present model	113.3	78.3	109.7	3.5
With 8% pre-strain						
Hardening model	Yield function	Solution method	$\theta_1(^{\circ})$	$\theta_2(^{\circ})$	$\rho_{sw}(mm)$	Average error %
		Experimental [25]	118.2	77.6	98.9	
ANK	Hill48	Previous model [19]	115.9	76.9	98.1	1.2
YU	Hill48	Present model	116.2	77.0	97.8	1.1

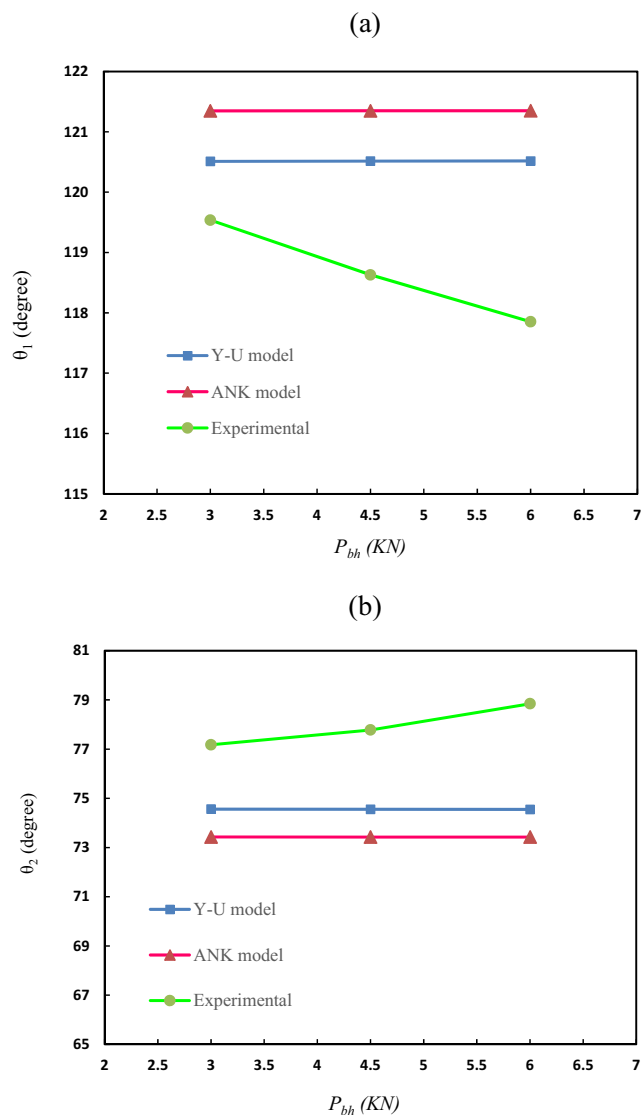


Fig. 11 The effect of blank holder force P_{bh} on the sheet springback based on the ANK [19] and present YU model in comparison with experimental data [26] **a** angle θ_1 and **b** angle θ_2

Calculation of critical sheet holder force

The ultimate strain determines bending capability of the sheet. An increase of holding force reduces the springback but causes sheet thinning and increase of the tensile strain. It is also possible that the tensile strain on the outer surface of the sheet exceeds the ultimate strain and creates initial cracks outside the sheet. The sheet strain has a maximum value at the outer surface of blank, which is bent around the die corner. The maximum value of the tangential strain ($\varepsilon_{\theta}^{max}$) can be calculated as follows:

$$\varepsilon_{\theta}^{max} = \frac{\bar{\varepsilon}_{lim} + \frac{t}{C_h} \bar{\varepsilon}_{yield}^{-pre}}{R_n} = \frac{R_o - R_n}{R_n} \tag{73}$$

Based on the Eq. (73), the value of the critical thickness will be obtained. By comparing the tensile force in different regions of the sheet, it can be seen that the tension in region III is the greatest. The maximum value of the sheet tensile force (F_{lim}) can be obtained based on the Eq. (61). Corresponding to Eq. (37) the maximum blank holder force can be obtained from:

$$P_{max} = \frac{F_{lim}}{\mu e^{\mu \frac{r}{2}}} \tag{74}$$

Results and discussion

This analytical model can be used for the analysis of two-dimensional stretch-bending process proposed in the Numisheet 2011 benchmark problem [24]. Since the side wall experiences bending, unbending and reverse bending, this problem is suitable to examine the ability of different hardening models to predict material mechanical behavior under the reverse loading.

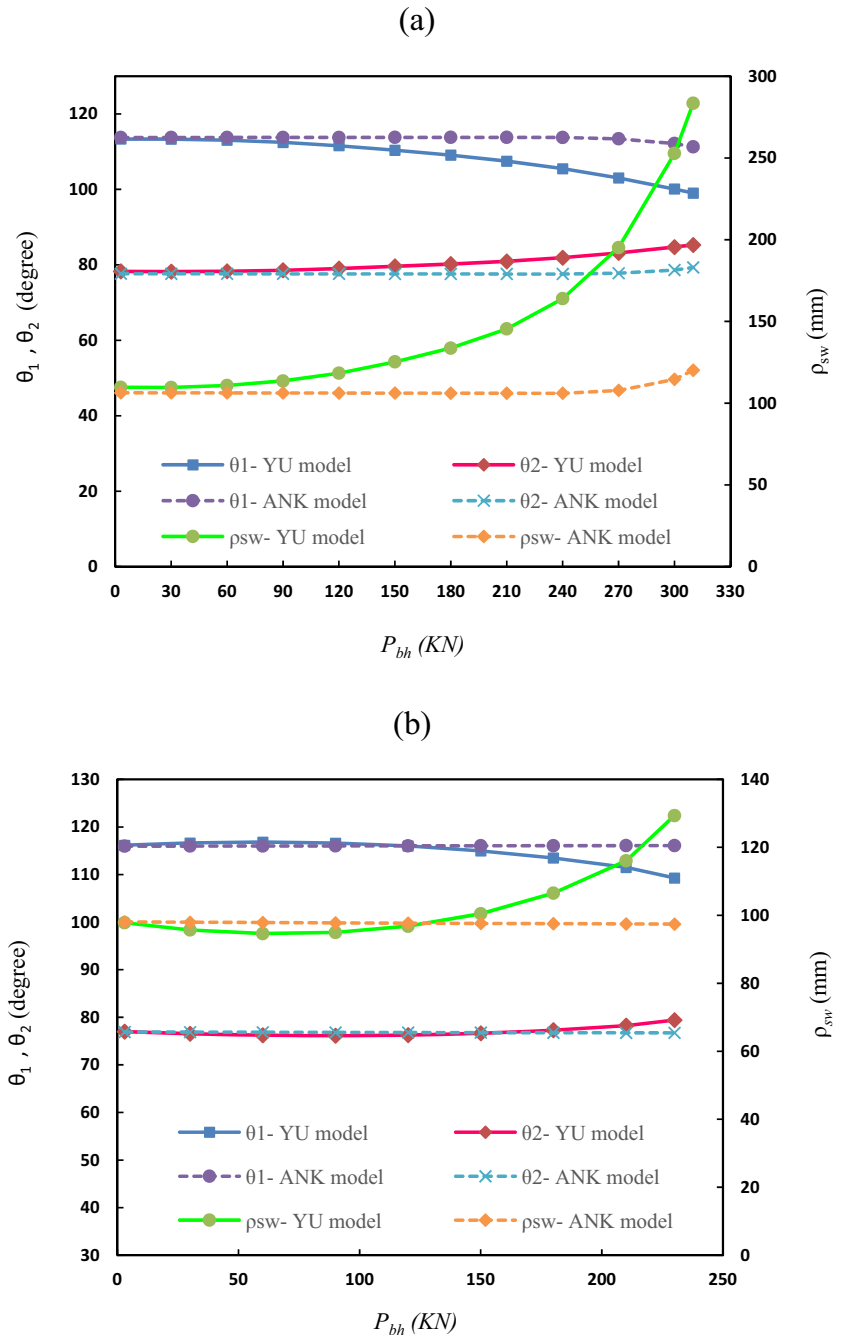
The geometry and dimensions of the U-shaped stretch-bending problem have been reported in the Numisheet2011 benchmark and are shown in Fig. 10. Dual-phase DP780 steel sheet with a thickness of 1.4 mm is used in this test. Two types of specimens are used for this test: one with the as-received

material (without pre-strain) and the other with pre-stretching by 8% in engineering strain along the rolling direction. Rectangular specimens were used with a width of 30 mm and 360 mm length. The pre-strained samples were first stretched along the rolling direction. The length of grip end is 25.0 mm, and then the specimen was cut-out from the central portion. The length of the sample after 8% pre-strain and trimming process is equal to 324 mm. During the forming process, the blank-holding force is equal to 2.94 kN and the punch speed is equal to 1 mm/s, while the punch stroke after the first contact between the punch and the sheet is equal to

71.8 mm. Moreover, the friction coefficient between the tools and sheet is equal to 0.1. According to Eq. (74), the maximum value of blank-holding force for the standard and the pre-strained blank is equal to 311.7 kN and 260.2 kN, respectively.

Comparisons of the springback parameters driven from current and previous models (see ref. [18, 19]) are illustrated in Table 2 with the experimental results, in order to validate our new model. All geometrical and mechanical parameters are the same as the Numisheet2011 benchmark 4. It can be seen that presented new model has less error in comparison with the previous type (ANK model) being closer to the

Fig. 12 The effect of blank holder force P_{bh} on the springback parameters prediction based on the ANK model [19] and present YU model for (a) blank without pre-strain and (b) with 8% pre-strain



experimental data. Also, it can be seen that the modified Yoshida-Uemori hardening model has more ability to describe the hardening behavior of the material in comparison with the ANK hardening model.

In our previous papers [18, 19], the effect of the blank holder force, blank thickness, anisotropy coefficient, pre-strain and hardening parameters on the springback have been investigated. To make continuity of the relation between springback results obtained from present and ANK model,

the blank holder force and work hardening stagnation are examined.

Figure 11(a) and (b) show the effect of blank holder force on springback of the as-received blank with 1 mm thickness for previous and present models, respectively. They are compared with experimental data [26]. It can be seen blank holder force almost does not affect the springback parameters predicted by analytical models while in the experimental results, the springback decreases gradually from the beginning.

Fig. 13 The effect of hardening parameter h on the springback parameters prediction. (a) blank without pre-strain and (b) blank with 8 % pre-strain

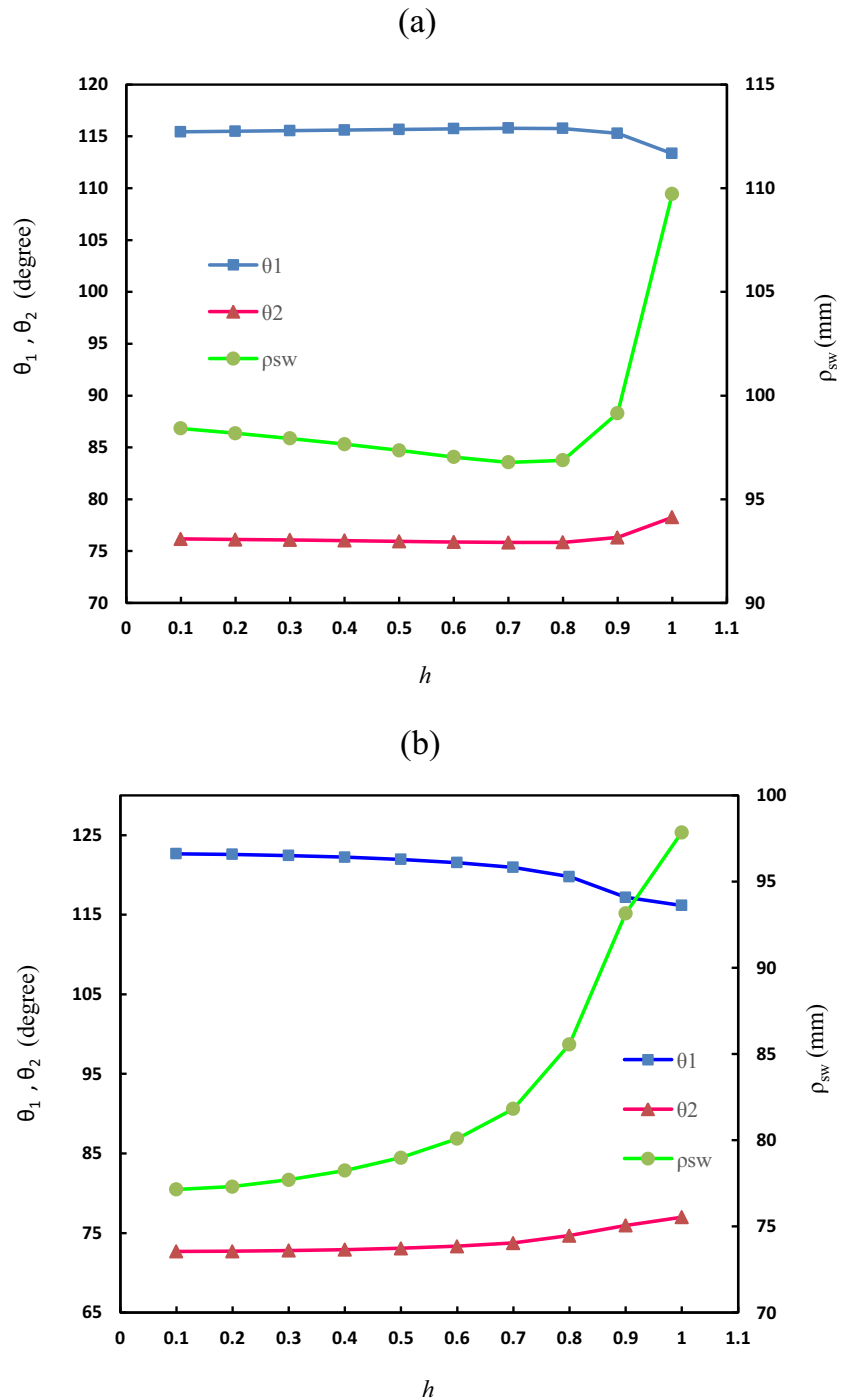


Figure 12(a) and (b) illustrates the effect of blank holder force on springback parameters of previous and present model respectively for as-received and pre-strained specimens. It can be seen that the blank holder force almost does not affect the springback parameters predicted by the previous model before it reaches 270 kN and springback decreases suddenly while in the present model the springback decreases gradually from the beginning. It can be seen that the sheet springback can be reduced by increasing the blank holder force.

Figure 13(a) and (b) illustrates the effect of work hardening stagnation parameter (h) on the springback measurements of the as-received and pre-strained specimens. It can be seen that increasing the parameter (h) almost does not affect over the springback of the as-received sample until reach value of 0.8. While for pre-strained specimen, the springback gradually decreases from the beginning.

Conclusion

A novel analytical model has been introduced here based on Hill48 yield criteria and plane-strain conditions to predict the springback of the U-shaped stretch-bending process explained in Numisheet2011 benchmark 4. Moreover, the plastic behavior is described based on the modified Yoshida-Uemori two surface hardening model. Also, the variation of the sheet thickness during the unloading process is neglected. This analysis is done for the as-received and pre-strained specimen to investigate the effect of blank holder force and work hardening stagnation. The obtained results show good agreement with the experimental data. This model can take into account the hardening characteristics of the material such as the Bauschinger effect, permanent softening, transient behavior, and work hardening stagnation in the reverse loading process. Also, the axes of material anisotropy are assumed to be orthogonal. The results obtained from the present model are compared with our analytical model published previously. It is seen that current results have fewer errors when both models are compared with the available experiments.

The effects of the work hardening stagnation and blank holder force on springback prediction are investigated. It can be seen that increase of the work hardening stagnation parameter (h) until value 0.8 almost does not affect the springback of the as-received specimen. But, in the case of pre-strained blank, it gradually decreases from the beginning. The increase of the blank holder force causes declining springback in the case of the as-received specimen. It can be seen this variation of springback is suddenly in the previous analytical model, while in present novel model, the change is gradual. During the last model for pre-strained blanks, the springback almost

has not variation with increasing the blank holder force while in this model, the variations are continuous.

Compliance with ethical standards

Conflict of interest The authors declare that they have no conflict of interest.

Publisher's Note Springer Nature remains neutral with regard to jurisdictional claims in published maps and institutional affiliations.

References

1. Yoshida F, Uemori T (2002) A model of large-strain cyclic plasticity describing the Bauschinger effect and work hardening stagnation. *Int J Plast* 18:661–686
2. Ghaei A, Green DE, Taherizadeh A (2010) Semi-implicit numerical integration of Yoshida–Uemori two-surface plasticity model. *Int J Mech Sci* 52:531–540
3. Ghaei A, Green DE (2010) Numerical implementation of Yoshida–Uemori two-surface plasticity model using a fully implicit integration scheme. *Comput Mater Sci* 48:195–205
4. Hu K-K, Peng X-Q, Chen J et al (2011) Springback prediction of automobile body panel based on Yoshida-Uemori material model [J]. *Mater Sci Technol* 6:9
5. ZHANG L, CHEN J, CHEN J (2012) Springback prediction of advanced high strength steel part based on Yoshida-Uemori hardening model. *Die Mould Technol* 3:4
6. Zhu YX, Liu YL, Li HP, Yang H (2013) Springback prediction for rotary-draw bending of rectangular H96 tube based on isotropic, mixed and Yoshida–Uemori two-surface hardening models. *Mater Des* 47:200–209
7. Kagzi SA, Gandhi AH, Dave HK, Raval HK (2016) An analytical model for bending and springback of bimetallic sheets. *Mech Adv Mater Struct* 23:80–88
8. Yi HK, Kim DW, Van Tyne CJ, Moon YH (2008) Analytical prediction of springback based on residual differential strain during sheet metal bending. *Proc Inst Mech Eng part C. J Mech Eng Sci* 222:117–129
9. Yang X, Choi C, Sever NK, Altan T (2016) Prediction of springback in air-bending of advanced high strength steel (DP780) considering young's modulus variation and with a piecewise hardening function. *Int J Mech Sci* 105:266–272
10. Zhang D, Cui Z, Chen Z, Ruan X (2007) An analytical model for predicting sheet springback after V-bending. *J Zhejiang Univ A* 8: 237–244
11. Parsa MH, Pishbin H, Kazemi M (2012) Investigating springback phenomena in double curved sheet metals forming. *Mater Des* 41: 326–337
12. Zhang LC, Lin Z (1997) An analytical solution to springback of sheet metals stamped by a rigid punch and an elastic die. *J Mater Process Technol* 63:49–54
13. Xue P, Yu TX, Chu E (1999) Theoretical prediction of the springback of metal sheets after a double-curvature forming operation. *J Mater Process Technol* 89:65–71
14. Pourboghra F, Chu E (1995) Springback in plane strain stretch/draw sheet forming. *Int J Mech Sci* 37:327–341
15. Zhang D, Cui Z, Ruan X, Li Y (2007) An analytical model for predicting springback and side wall curl of the sheet after U-bending. *Comput Mater Sci* 38:707–715

16. Nanu N, Brabie G (2012) Analytical model for prediction of springback parameters in the case of U stretch–bending process as a function of stresses distribution in the sheet thickness. *Int J Mech Sci* 64:11–21
17. Jiang H-J, Dai H-L (2015) A novel model to predict U-bending springback and time-dependent springback for an HSLA steel plate. *Int J Adv Manuf Technol* 81:1055–1066
18. Zajkani A, Hajbarati H (2017) An analytical modeling for springback prediction during U-bending process of advanced high-strength steels based on anisotropic nonlinear kinematic hardening model. *Int J Adv Manuf Technol* 90:349–359
19. Zajkani A, Hajbarati H (2017) Investigation of the variable elastic unloading modulus coupled with nonlinear kinematic hardening in springback measuring of advanced high-strength steel in U-shaped process. *J Manuf Process* 25:391–401
20. Eggertsen P-A, Mattiasson K (2009) On the modeling of the bending–unbending behavior for accurate springback predictions. *Int J Mech Sci* 51:547–563
21. Lee J-Y, Lee J-W, Lee M-G, Barlat F (2012) An application of homogeneous anisotropic hardening to springback prediction in pre-strained U-draw/bending. *Int J Solids Struct* 49:3562–3572
22. Eggertsen P, Mattiasson K, Larsson M (2011) A comprehensive analysis of benchmark 4: pre-strain effect on springback Of 2D draw bending. In: *AIP Conf. Proc.* AIP, pp 1064–1071
23. Hill R (1998) *The mathematical theory of plasticity*. Oxford University Press, New York
24. Chung K, Kuwabara T, Verma R, Park T (2011) Numisheet 2011 Benchmark 4: Pre-strain effect on spring-back of 2D draw bending. In: *Proc. 8th NUMISHEET Conf.* Seoul, Korea. pp 171–175
25. Zang S, Lee M, Kim JH (2013) Evaluating the significance of hardening behavior and unloading modulus under strain reversal in sheet springback prediction. *Int J Mech Sci* 77:194–204
26. Sae-Eaw N, Thanadngarn C, Sirivedin K et al (2013) The study of the springback effect in the UHSS by U-bending process. *King Mongkut's Univ Technol North Bangkok. Int J Appl Sci Technol* 6:19–25